

## **Known instrumental effects that affect the OML1B product of the Ozone Monitoring Instrument on EOS Aura**

Marcel Dobber

Last update 02 June 2008.

### **References:**

- RD01 GDPS Input / Output Data Specification (IODS) Volume 2: Level 1B output products and metadata, SD-OMIE-7200-DS-467, issue 5, 25 August 2006.
- RD02 G. H. J. van den Oord, J. P. Veefkind, P. F. Levelt, M. R. Dobber, Level 0 to 1B processing and operational aspects, IEEE Trans. Geosc. Rem. Sens. **44** (5), pp 1380-1397 (2006).
- RD03 GDPS Input / Output Data Specification (IODS) Volume 4: Operational Parameters File Specification , SD-OMIE-7200-DS-488, issue 5, 25 August 2006.
- RD04 Transient signal flagging algorithm definition for radiance data, TN-OMIE-KNMI-717, issue 2, 12 July 2005.
- RD05 Transient signal flagging algorithm definition for non-radiance data, TN-OMIE-KNMI-718, issue 2, 12 July 2005.
- RD06 OMI GDPS algorithm to correct for wavelength shifts due to inhomogeneous slit illumination, TN-OMIE-KNMI-680, issue 1, 17 January 2005.
- RD07 In-flight wavelength assignment: correcting for inhomogeneous slit illumination, TN-OMIE-KNMI-692, issue 1, 17 March 2005.
- RD08 Reducing along-track stripes in OMI-Level 2 products, TN-OMIE-KNMI-785, version 1.0, 13 March 2006.
- RD09 Ozone Monitoring Instrument calibration, M. R. Dobber, R. J. Dirksen, P. F. Levelt, G. H. J. van den Oord, R. Voors, Q. Kleipool, G. Jaross, M. Kowalewski, E. Hilsenrath, G. Leppelmeier, J. de Vries, W. Dierssen, N. Rozemeijer, IEEE Trans. Geosc. Rem. Sens. **44** (5), pp 1209-1238 (2006).
- RD10 Method of calibration to correct for cloud-induced wavelength shifts in the Aura satellite's Ozone Monitoring Instrument, R. Voors, M. Dobber, R. Dirksen, P. Levelt, Applied Optics, Vol. **45**, No. 15, 3652-3658.
- RD11 Validation of Ozone Monitoring Instrument level-1b data products, M. Dobber, Q. Kleipool, R. Dirksen, P. Levelt, G. Jaross, S. Taylor, T. Kelly, L. Flynn, G. Leppelmeier, N. Rozemeijer, submitted to J. Geophys. Res. special issue on EOS-Aura validation.
- RD12 The high-resolution solar reference spectrum between 250 and 550 nm and its application to measurements with the Ozone Monitoring Instrument, M. Dobber, R. Voors, R. Dirksen, Q. Kleipool, P. Levelt, submitted for publication to Solar Physics.
- RD13 Use of Antarctica for validating reflected solar radiation measured by satellite sensors, G. Jaross and J. Warner, submitted to J. Geophys. Res. special issue on EOS-Aura validation.
- RD14 Ozone Monitoring Instrument geolocation verification, M. Kroon, R. Dirksen, M.R. Dobber, submitted to J. Geophys. Res. special issue on EOS-Aura validation.

### **General**

Applicable to GDPS version 1.0.0.

Applicable to collection 3 data stream.

Applicable to Time Dependent Operational Parameter Files (TDOPFs).

Applicable to orbit number 1 and higher (15 July 2004 and later).

First public release of OMI level-1b data.

The detailed GDPS operational 0-1 processor details are not discussed here, the reader is referred to RD01-RD03. The level-1b output products and metadata is described in detail in RD01. More details on the OMI instrument design characteristics and on the on-ground and in-flight calibration details are given in RD09.

## General-1)

Proton radiation damage: Background correction.

Proton-induced radiation damage on the CCD detectors may lead to the following effects observed in unbinned pixels:

- 1) Dark current increase by a factor of at least 4-5 relative to pre-launch values.
- 2) RTS behaviour after the pixel has been hit (see below: RTS).

Proton hits on CCD detector pixels do not necessarily have to lead to any or both of the above effects. It is more likely that the proton hit will cause a transient spike that will not result in lasting damage (see below: transients).

The effects in the unbinned pixels obviously also transfer into the behaviour of the binned pixels than contain the unbinned pixels that were hit by protons. The rate at which pixels are hit in the UV and VIS channels (image and storage sections of the CCD detectors) is about 29 unbinned pixels per day per detector per region. The damage occurs mostly via trapped protons in the South-Atlantic Anomaly (SAA) and in the radiation belts close to the north and south poles. The aluminium shielding with an average thickness of about 29 mm is not capable of stopping high-energetic protons (e.g. >100 MeV) before they reach the CCD detectors. In addition, high-energetic protons may create secondaries in the aluminium shielding, which in turn may yield additional damage to the CCD detectors.

Both effects require frequent updates of the background images contained in the Operational Parameter File (OPF) for the background subtraction algorithm in the 0-1 data processor. The OPF contains the calibration data as required by the GDPS. For the collection 3 data stream discussed here the background images are updated dynamically once per day. For orbit numbers 1 to 16306 (15 July 2004 to 8 August 2007) the background images are taken from the same day as the light measurements (earth or sun). For later orbit numbers and dates the background images are also updated dynamically once per day, but using the background image data from 2-3 days before the light measurements. The resulting background subtraction is very close to the optimal correction, but the correction can never be perfect for RTS pixels (see below). Imperfectly background corrected pixels may show up as smaller or larger spikes in the background corrected images, or the imperfectly background corrected pixels may show up as a higher noise in the background corrected image.

## General-2)

Proton radiation damage: Random Telegraph Signals (RTS)

See also above (proton radiation damage: background correction).

After a pixel has been hit by a proton it may develop RTS, i.e. the response of the pixel without illumination jumps in time between at least two signal levels. Of course, this also occurs when the pixel is illuminated. The time periods between the jumps can be from seconds to even days. The amplitude between the jumps can also vary greatly between the original dark current and about 4-5 times the original dark current. The different signal levels can be more or less stable, or show exponential decrease or increase with time. It can not be predicted what behaviour a pixel will show when it is hit. It is only possible before the pixel is hit to express statistically what the chance is that a pixel will show certain behaviour. Once a pixel has in fact been hit, it is possible to express statistically what the chance is that it will be at a certain signal level. It is not possible to predict with 100% certainty what the signal level of that specific pixel will be. The RTS behaviour makes the background correction algorithm less accurate. Even with the most recent background images in the OPF, it is not possible to correct for the background signal of RTS pixels with the same accuracy as for pixels that do not show RTS, because as a result of the statistical nature of the RTS it is not possible to predict the signal level of such a pixel beforehand. When the RTS is too severe, the pixel may become practically unusable.

(Binned) pixels that show too severe RTS have been flagged in the level-1 data by the 0-1 data processor (RTS warning pixel quality flag) by using an unbinned map to identify severe RTS pixels. These flags have been set conservatively in order to avoid flagging a large percentage of the data. However, it is recommended to exclude flagged RTS pixels from subsequent data analysis. After 3 years in orbit about 1% of all binned pixels has been flagged with an RTS warning.

In addition, radiation damage may cause pixels to be flagged as bad (bad pixel quality flag). This happens when the dark current becomes too high, when the pixels always gives zero response (disconnected pixel), or when the pixel response is too low in a White Light Source (WLS) measurement. After 3 years in orbit about 1% of all binned pixels has been flagged bad.

The RTS warning and bad flags are taken from the Bad and Dead Pixel Map (BDPM) in the OPF. For the collection 3 data stream discussed here the BDPMs are updated dynamically once per day using the Time Dependent OPF system (TDOPF). For orbit numbers 3457 to 16306 (9 March 2005 to 8 August 2007) the BDPMs are taken from the same day as the measurements that are being processed. For later orbit numbers and dates the BDPMs are also updated dynamically once per day, but using the BDPM from 3 days before the measurements that are being processed. For orbit numbers lower than 3457 (before 9 March 2005) the BDPM from 9 March 2005 is used.

#### General-3)

Proton radiation damage: Transients.

See also above (proton radiation damage: background correction).

Pixels that are hit by protons or other particles can show subsequent permanent or longer lasting damage effects. However, it is more likely that pixels are hit and only show significantly increased signal during one readout, a so-called transient spike. In the readouts following the one in which the hit occurred no lasting effects of the hit can be found. In the GDPS dedicated algorithms have been developed for radiance and irradiance measurement data in order to identify and flag these transient spikes (RD04 and RD05). In case a transient is detected the pixel quality flag (bit number 3) for that detector pixel is raised. In certain regions on the earth the number of transient spikes is higher than in the remaining regions, e.g. in the radiation belts close to the north and south poles and in the south Atlantic anomaly.

#### General-4)

Stripes (variability with viewing angle) in various level 2 data products originating from level 1 radiance and irradiance data.

Several level 2 data products may show residual features as a function of swath angle, so-called stripes. These features can persist over an entire orbit or even over more orbits. An extreme example is shown in figure 1 below. Although the stripes in the level 2 data products must originate from swath-angle-dependent features in the level 1 data, they are not easily visible in the level 1 data.

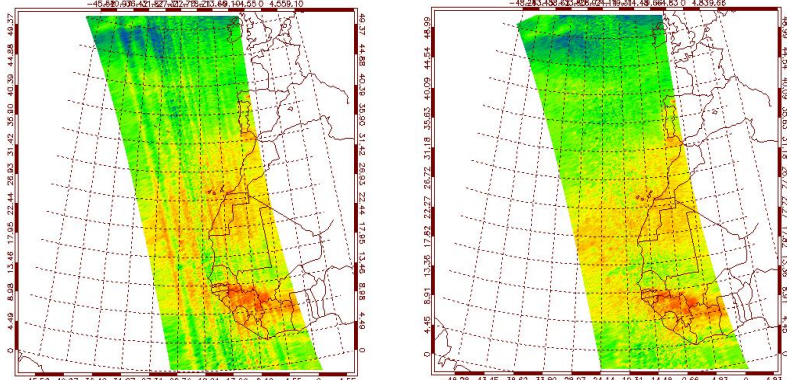


Figure 1: Nitrogen dioxide level 2 data product result for a specific orbit over west Africa. The left figure shows the (exaggerated) along-track stripes at certain cross-track swath viewing angles. The right figure shows the same orbit with reduced stripes.

The stripe phenomenon was carefully investigated by investigating the impact on the nitrogen dioxide retrieval in the visible channel. The results are given in RD08. It was shown that the amplitudes of the stripes can be reduced by a factor of 3-4 when images from the same day are used for the background correction of the light images. This optimised background correction has

been implemented in the collection 3 data discussed here using the time-dependent OPF (TDOPF) system. The persisting stripes over an orbit originate from the irradiance product used to calculate the earth reflectance (ratio earth radiance / sun irradiance) for the orbit under investigation. For collection 3 a considerable improvement in the trace gas retrievals and in the ozone products has been observed as compared to collection 2.

These stripes can be further reduced by averaging multiple solar irradiance products from different days. No specific level-1b data products with averages are made available: the averaging is the responsibility of the level-1b data user.

#### General-5)

##### Gain switching columns.

The CCD can have in the column (wavelength) dimension up to four regions with different electronic gain settings. These regions are separated by up to three gain switching column, that can be located in columns in the full-performance range of the instrument. During on-ground testing it has been observed that 2-3 columns higher than the gain switching columns show electronic settling effects. These effects are corrected for in the GDPS, but the result after correction may still be less accurate than columns located more than three columns higher than the gain switching columns. The locations of the gain switching columns can be found in the level-1b data products.

#### General-6)

##### Pixel-to-pixel Response Non-Uniformity (PRNU).

The CCD detectors show pixel-to-pixel response non-uniformity variations of up to 5%. These variations are more or less diagonal over the CCD detectors and are most pronounced in the ultraviolet wavelength range (up to 5%) and far less pronounced in the visible wavelength range (< 0.1%). The effect is corrected for in the 0-1 data processing, but the correction is not perfect. Residual errors of up to 0.1-0.2% may be observed in some cases in the individual radiance or irradiance spectra. The PRNU effect or residual errors cancel to a large degree when the ratio of radiance over irradiance data is calculated.

#### General-7)

##### Entrance slit irregularities.

The entrance slit of the OMI spectrometer has a nominal width of 300  $\mu\text{m}$  and a length of about 40 mm and is known to show width variation along the length of the slit of up to several percent. The radiometric effect is sufficiently wavelength independent, but manifests itself differently in the UV1, UV2 and VIS optical subchannels. The effect is corrected for in the 0-1 data processing, but the correction is not perfect. Residual errors of up to 0.1-0.2% may be observed in some cases in the individual radiance or irradiance spectra. The slit irregularity effect or residual errors cancel to a large degree when the ratio of radiance over irradiance data is calculated.

#### General-8)

##### Optical degradation.

During the OMI mission the optical throughput of the instrument will start to degrade at some point. The on-board diffusers and the primary telescope mirror are among the most likely candidates to show evidence of degradation first. Once significant degradation starts to occur it will take some time to describe past degradation and try to predict future degradation accurately and before these characterisation data are fully implemented in the operational data processing chain.

However, at this point in time no significant degradation (i.e. larger than 1%) has been observed in either the earth or the sun mode in the wavelength range 264-504 nm.

Monitoring the degradation of the primary telescope mirror in the earth mode is difficult, because no known and stable illumination scenes or sources over the full OMI wavelength range can be used to accomplish this, unlike for example the internal white light source mode or the sun modes. One needs to rely on ground scenes that are sufficiently well understood. Current indications are that the primary telescope mirror has not degraded significantly (i.e. more than 1%).

## **Level 1 irradiance data**

### **Irradiance-1)**

Irradiance goniometry correction.

The irradiance calibration depends on the azimuth (seasonal dependence) and elevation (orbital position dependence) angles, as well as on the viewing angle (row), wavelength (column) and on-board diffuser employed for the solar measurement. The currently implemented calibration key data in the OPF for the quartz volume diffuser and the algorithm in the 0-1 data processor for the irradiance goniometry correction are not perfect. Row dependent errors of up to 0.5% in UV1 and UV2 and up to 0.2% in VIS can remain after correction for azimuth angles below 31.0 degrees. For azimuth angles larger than 31.0 degrees and binned row numbers smaller than 15 in UV2 the accuracy of the irradiance correction for the volume diffuser decreases to 1%. When the azimuth angle exceeds 31.2 degrees larger irradiance goniometry calibration errors may result from extrapolation errors with respect to the in-flight measurement data used to derive the calibration constants currently used in the OPF.

### **Irradiance-2)**

Diffuser spectral and spatial features.

It has been known already since the on-ground performance verification and calibration that the on-board diffusers show spatial (row-dependent) and spectral (column dependent) features that change with azimuth and elevation angles of incidence on the diffuser surface. The spatial features have amplitudes of up to 4% for the aluminium diffusers and 0.1% for the quartz volume diffuser. The spectral features have periods of typically 5-10 nm and amplitudes of up to typically 4% for the aluminium diffusers and 0.1% for the quartz volume diffuser. The quartz volume diffuser is used for the daily solar measurements that are processed by the 0-1 data processor into the official level-1b irradiance product. The solar measurements via the aluminium diffusers are performed once per week (regular aluminium diffuser) and once per month (backup aluminium diffuser). These measurements via the aluminium diffusers are stored only in the level-1b calibration files. The performance of the aluminium diffusers in terms of spectral and spatial features is not critical for users of OMI level-1b data products until these diffusers are needed to correct for potential degradation of the quartz volume diffuser. In September 2007, more than three years after launch, this is not yet the case.

### **Irradiance-3)**

Irradiance absolute radiometric calibration.

UV2-VIS.

The irradiance absolute radiometric calibration has been calibrated by comparing the measured irradiance with a high-resolution solar reference spectrum convolved with the OMI spectral slit functions, that have been accurately calibrated on the ground. Any deviations from one in the ratio of these two spectra can result from inaccuracies in:

- The spectral assignment in the measured irradiance.
- The spectral slit functions.
- The high-resolution solar reference spectrum.
- The irradiance absolute radiometric calibration.

The current result is shown in figure 2 for the quartz volume diffuser.

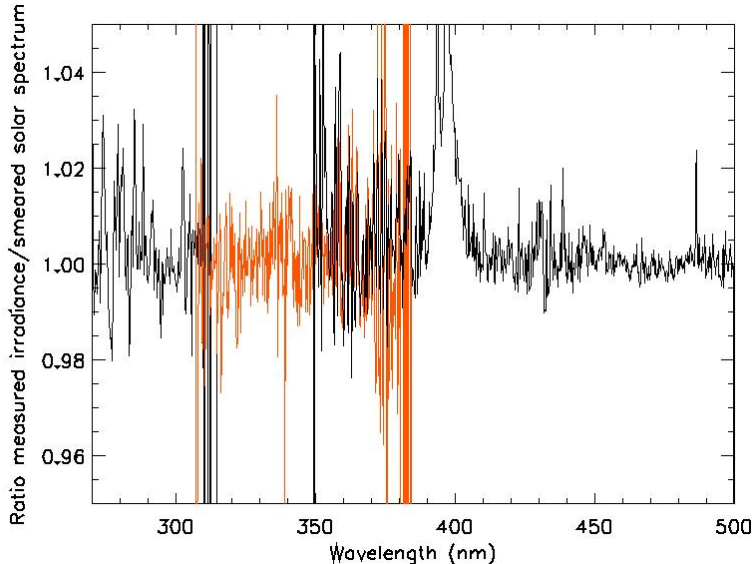


Figure 2: Ratio measured irradiance / high-resolution solar spectrum convolved with spectral slit functions for orbit 2465 (31 December 2004) for the quartz volume diffuser.

Some residual structure in the order of 1-2% remains. The Call lines show up with an amplitude of about 3-4%, which can be tentatively attributed to differences in the high-resolution solar reference spectrum with regards to solar activity in combination with errors in the spectral slit functions.

Comparisons have also been made to existing solar reference spectra measured by other satellite instruments. The agreement of the OMI level-1b irradiance data product with these other available literature irradiance spectra is within 4% [RD11, RD12].

The swath angle dependence of the irradiance as measured over the on-board quartz volume diffuser is currently calibrated to an accuracy of better than 0.3% (see figure 3) for all wavelengths in the full-performance range of the instrument.

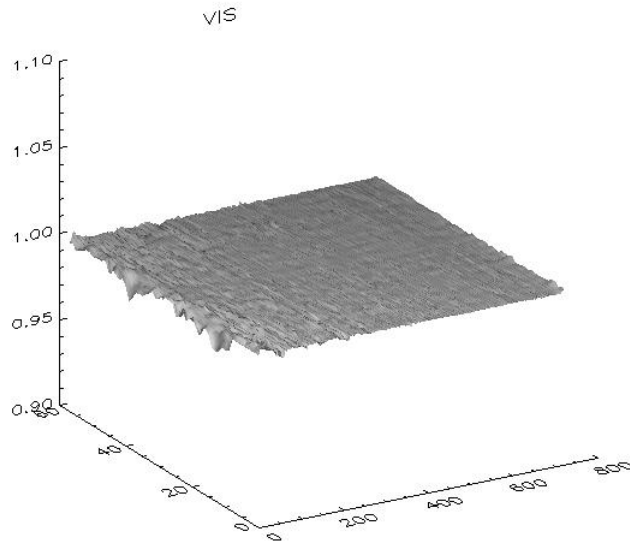


Figure 3: Irradiance swath angle dependence in the VIS channel for orbit 2465 (31 December 2004) for which the azimuth angle is nominal (25.75 degrees). The horizontal axes are the column number (spectral dimension) and row number (viewing angle dimension), the vertical axis is the measured response.

#### Irradiance-4)

##### Spectral assignment.

The current accuracy of the spectral assignment for sun spectra is about 0.02 pixel in UV1 and about 0.01 pixel in UV2 and VIS. A difference of up to 0.01 pixel between the wavelength calibrations from the sun spectra and from the earth spectra has been observed in UV2 and VIS. The reason for this difference is currently not understood.

#### Irradiance-5)

##### Missing data in the level-1b irradiance data product.

The data in the level-1b irradiance data product is the solar measurement data as measured over the on-board quartz volume diffuser. During a solar measurement of about 2 minutes the elevation angle on the diffuser changes as a result of the orbital movement of the satellite. The GDPS averages all measurements in a predefined range of solar elevation angles on the on-board diffuser. The currently used range is between -3.0 degrees and +3.0 degrees. Averaging is performed to improve the signal-to-noise ratio and to reduce the diffuser features as much as possible. However, if a pixel is flagged bad for all measurements in the elevation angle range, for example because the pixel is flagged bad in the Bad and Dead Pixel Map (BDPM), no data is taken into account for that pixel and the final result is that a fill-value is written in the level-1b irradiance data product and the so-called 'missing' flag is set for that pixel. If more and more pixels are flagged bad as a function of time, the number of missing data pixels in the level-1b irradiance data product will increase accordingly. Note that these pixels can not be used for scientific studies, because they have been marked bad. See also the General-1 and General-2 points above.

If, on the other hand, a transient pixel is observed for only one or a few solar frames, these transient pixels are not taken into account in the calculated average, and an average based on the valid (non-transient pixel) observations is available in the level-1b irradiance data product. The pixel quality flag is set to 'transient' to indicate that for this pixel in at least one of the individual frames a transient was detected. If this pixel quality flag is set for the irradiance data product, the pixel can still be used without caution. If the transient flag is set for the radiance data product, the pixel shall not be used.

#### Irradiance-6)

##### Irradiance signal-to-noise.

In the irradiance mode the light enters the instrument via a solar mesh with 10% transmission, an on-board reflection diffuser and a folding mirror. As explained in the above paragraph (Irradiance-5) the level-1b irradiance data product for one day is the average of typically 60-70 individual solar measurements over the quartz volume reflectance diffuser. As a result of the combination of the attenuation of the mesh and the low reflectivity of the quartz the signal levels of the individual measurements are quite low. The signal-to-noise of the irradiance data product for one day is also correspondingly quite low. If the level-1b irradiance data product from a single day is used the signal-to-noise of that irradiance data product can not be ignored when the ratio of radiance and irradiance (earth reflectance) is considered.

On the other hand, the radiometric and spectral stability are very good over long time periods. So, if the data application allows it, it is recommended to average various daily level-1b solar irradiance data products in order to improve the signal-to-noise.

## Level 1 radiance data

### Radiance-1)

Spectral stray light correction.

The spectral stray light correction algorithm, that is currently implemented in the 0-1 data processor, calculates the source contributions by using measurement data from all viewing directions (rows) and applies the correction to the target region with the same magnitude and wavelength dependence for all rows in UV1. For UV2 and VIS the spectral stray light correction is performed with the source contributions and the target positions at the same viewing angle. In this way inhomogeneous scenes are properly corrected in the UV2 and VIS channels. Investigations have shown that this viewing angle dependence is not required for the spectral stray light correction in the UV1 channel, where the spectral stray light correction is most crucial, because the spectral stray light is highest as compared to the useful signal. The reason for this is that the viewed scenes in UV1 are quite homogeneous, because for wavelengths lower than 300 nm the ground and clouds are not observed. It turns out that the stray light distributes more or less homogeneously over all rows in the target region for the UV1 subchannel. Although the spectral stray light correction algorithm is quite sophisticated and properly accounts for all known instrumental stray light dependencies it is probable that the correction will not work perfectly for all observed ground scenes and for all types of stray light (including all spatial, or viewing angle dependent, stray light effects). For highly inhomogeneous ground scenes it is therefore not unlikely that residual spectral stray light correction inaccuracies of a few percent may remain.

### Radiance-2)

Radiance absolute radiometric calibration.

The radiance absolute radiometric calibration can not be calibrated as straightforwardly as the irradiance, because no accurate comparison standards are readily available. For this reason it was decided to start with the instrument Bi-directional Scattering Distribution Function (BSDF, basically the ratio of the radiance and irradiance radiometric calibrations) as calibrated on the ground. The absolute central-row (nadir viewing direction) BSDF was calibrated accurately (within 1%  $1\sigma$ ) on the ground. The inaccuracies in the swath angle dependence of the BSDF are larger. These inaccuracies transfer also to the swath angle dependence of the earth radiance and reflectance (ratio radiance / irradiance). On the ground the inaccuracies of the BSDF (including swath angle dependence) were considerably larger in the UV1-UV2 and UV2-VIS channel overlap regions as a result of the low instrument throughputs in these wavelength regions.

From detailed analysis on the radiance from ice it was observed that the central row (nadir) earth reflectance in-flight measurement data and the central row (nadir) earth radiance in-flight measurement data were 2.5% too low in the UV2 and VIS channels. In the collection 3 data discussed here this has been corrected for all channels (UV1, UV2, VIS). The same ice radiance analysis and investigations on the global distribution of the total column ozone as a function of swath angle revealed that the swath angle dependence of the earth reflectance and the earth radiance was off by several percent in the UV2 and VIS channels. Using the results from these analyses on in-flight measurement data the swath angle dependence of the earth reflectance and radiance was corrected in all channels (UV1, UV2, VIS). The correction factors that have been used are shown in figure 4. Although the ice radiance analysis provides no direct results for the UV1 channel it was decided to correct the radiance swath angle dependence in UV1 with the results as found for the UV2 channel, fitted with a second order polynomial. The resulting correction factor for UV1 is also shown in figure 4. Note that the spatial coverage in the UV1 channel is half of coverage in the UV2 and VIS channels.

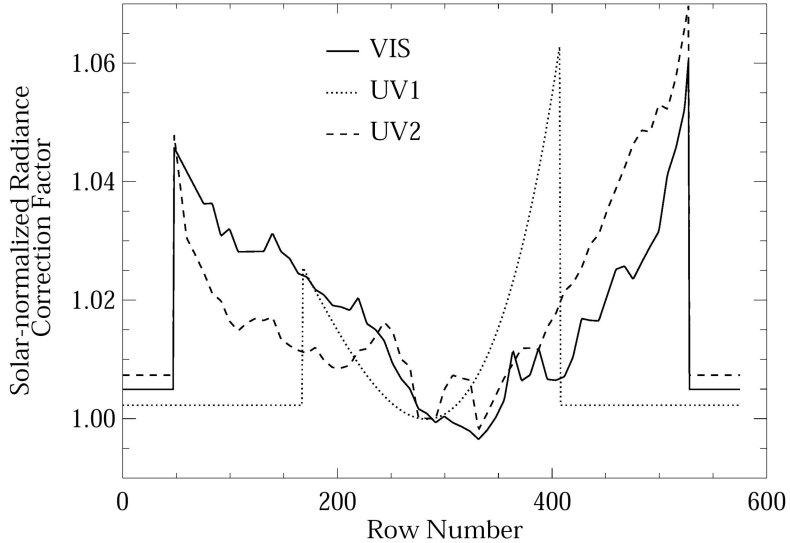


Figure 4: Final correction from ice radiances applied to detector rows for each channel. These corrections have been applied to the radiometric radiance calibration data in the OPF for collection 3.

Subsequent comparisons of the OMI radiance swath angle dependence at different wavelengths in the UV1 channel with MLS have revealed that differences of up to 5% occur (see figure 5). These differences are more or less independent of the wavelength in the UV1 channel. This difference has not yet been corrected in the collection 3 data. Since the swath angle dependence of the irradiance is expected to better than 0.3% (see figure 3), the inaccuracies in the radiance product are expected to transfer directly into the earth reflectance.

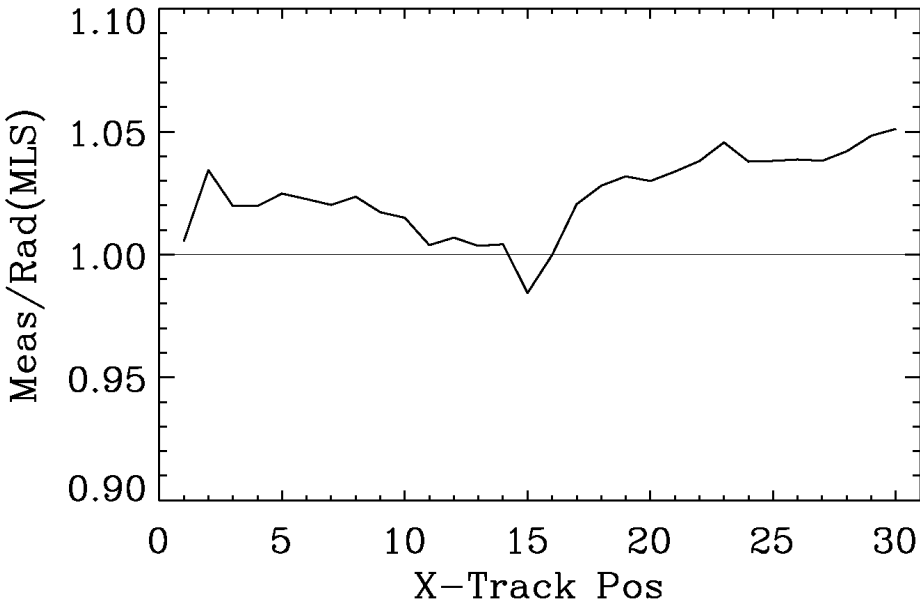


Figure 5: Ratio of measured OMI radiance and MLS radiance as a function of the swath angle in the UV1 channel at 287.6 nm. The result is more or less representative also for other wavelengths in the UV1 channel.

Given the above the central row absolute radiance is expected to be accurate to within about 2% ( $1\sigma$ ). The swath angle dependence of the radiance is also expected to be accurate to within about 2% ( $1\sigma$ ) for the UV2 and VIS channels and to within about 5% ( $1\sigma$ ) for the UV1 channel. More detailed analyses and comparisons using in-flight data will be performed in the future to improve these accuracies.

#### Radiance-3)

##### Geolocation.

In RD14 the OMI geolocation assigned to individual pixels in the VIS channel in the level-1b radiance product was found to be accurate to about 1 km in both latitude and longitude on average over the year 2005 without any clear seasonal dependence. A similar accuracy is expected for the UV1 and UV2 channels. The geolocation assigned to individual OMI ground pixels is sufficiently accurate to support scientific studies of the smallest details as observed from OMI satellite data products.

However, from on-ground measurements it is known that the line of sight between the flight direction can differ between UV1-UV2-VIS by as much as 0.10-0.15 degrees, corresponding to about 1.2-1.8 km at the central nadir position. The UV2 channel looks 'ahead' of the UV1 and VIS channels.

#### Radiance-4)

##### Interchannel discontinuities.

In some cases interchannel discontinuities of several percent can occur in the earth reflectance data, i.e. the ratio earth radiance over sun irradiance. This originates from the earth radiance data. Figure 6 shows some representative examples.

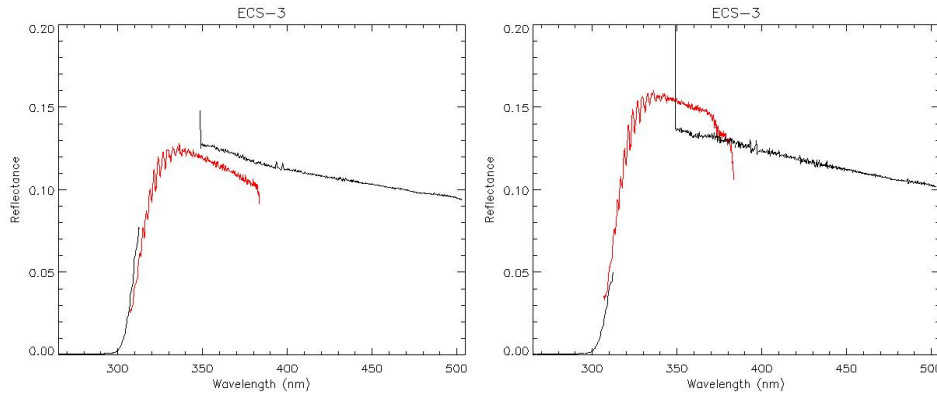


Figure 6: Example of interchannel discontinuities in the reflectance. The left panel shows a negative jump (image 754, row 21 for UV1 and 42 for UV2 and VIS), the UV2 channel lies below the VIS channel. The panel on the right shows a positive jump (image 754, row 20 for UV1 and 40 for UV2 and VIS). The data were taken from orbit 3760 (30 March 2005), the solar spectrum was taken from orbit 3831 (4 April 2005).

Further investigation reveals that such interchannel discontinuities may be related to pronounced scene changes in the flight direction, for example going from ice to ocean or vice versa, or flying over clouds. However, the correlation between the scene inhomogeneities in the flight direction and the appearance of the interchannel discontinuities in the reflectance is not well-behaved. Currently the origin of the discontinuity phenomenon is not understood.

#### Radiance-5)

##### Spectral assignment.

The current accuracy of the spectral assignment for both sun and earth spectra is about 0.02 pixel in UV1 and about 0.01 pixel in UV2 and VIS. For the earth spectra a correction is applied to the wavelength assignment to account for potential scene inhomogeneity (mostly originating from clouds) in UV2 and VIS. This correction can be as large as 0.5 pixel, depending on the scene

inhomogeneity (RD06, RD07, RD10). For UV1 the correction is not applied, because the observed scenes are sufficiently homogeneous. When the correction is applied in UV2 or VIS, this is indicated by one of the pixel quality flags in the level-1b data product.

A difference of up to 0.01 pixel between the wavelength calibrations from the sun spectra and from the earth spectra has been observed in UV2 and VIS. The reason for this difference is currently not understood.

The pixel wavelengths near the very ends of the orbits can for some measurements shift by a large number, 4 to 14 nm, and then back, between measurements: for such measurements the wavelength assignment is wrong. This may occur for measurement pixels for which the signal levels are very low. The effect may cause the wavelength to be not monotonically increasing with column number.

In addition, the wavelength correction for inhomogeneous scenes is not applied in the UV2 or VIS channels when the so-called small-pixel column pixel, that is used to estimate the scene inhomogeneity, has been flagged bad in the same channel. This will be corrected to some extent in a future release of the GDPS: when possible and necessary (i.e. when the small pixel column has been flagged as bad) the small pixel column from the UV2 channel will be applied to the VIS channel and vice versa in order to apply the wavelength correction for inhomogeneous ground scenes.

#### Radiance-6)

Anomaly at binned row numbers 53 and 54 in the UV2 channel and row 53 in the VIS channel (zero based) in the global earth measurements (binning factor 8).

Between 25 and 27 June 2007 a change occurred in the OMI instrument in the rows mentioned above. A decrease in the radiance signal of about 20-30% under illuminated conditions is observed over the complete illuminated part of the orbit. All columns (wavelengths) in the UV2 and VIS channels are affected by this effect. The anomaly seems to be more or less stable after 27 June 2007. The data before 25 June 2007 is much less affected by the row anomaly. The anomaly is currently under investigation and also if a correction for the effect can be implemented in the level-1b data. No correction has been implemented at the moment. It is recommended not to use the affected rows for now. If they are used anyhow, care should be taken in the interpretation of the results.

#### Radiance-7)

Anomaly at binned row numbers 18-21 in the UV1 channel and at binned row numbers 38-41 in the UV2 and VIS channels (zero based) in the global earth measurements (binning factor 8).

Since 11 May 2008 a signal suppression has been observed in the above rows for the UV2 and VIS channels (signal increase for the UV1 channel in the above rows), but only for northern latitudes, at Solar Zenith Angles (SZAs) larger than 44.0 degrees for the affected rows. For data products that are sensitive to very small signal changes the effect can already be observed starting at SZA larger than 34.0 degrees.

The anomaly is currently under investigation and also if a correction for the effect can be implemented in the level-1b data. No correction has been implemented at the moment. It is recommended not to use the affected rows at the latitudes and SZAs specified above for now. If they are used anyhow care, should be taken in the interpretation of the results.

## Earth reflectance data

The individual radiance and irradiance data products may contain a number of artefacts that are residuals of corrections in the 0-1 data processing that are not perfect. In many cases (e.g. PRNU, slit irregularity) such corrections are exactly the same for the radiance and the irradiance data products and when the ratio of radiance over irradiance (called the earth reflectance) is calculated potential non-optimal corrections cancel. This implies that the derived earth reflectance data product is in many aspects more accurate than the individual radiance or irradiance data products. Evaluations and comparisons on the reflectance data have shown that the absolute earth reflectance for the nadir viewing direction is currently accurate to about 2% ( $1\sigma$ ). The swath

angle dependence of the reflectance appears to be accurate also to within 2% ( $1\sigma$ ) for the UV2 and VIS channels and to within 5% ( $1\sigma$ ) for the UV1 channel (see also radiance-2 above). More detailed analyses and comparisons using in-flight data will be performed to improve these accuracies further.

Note that the earth reflectance data is not an official output data product of the 0-1 data processor. The earth reflectance data can be calculated by the data user from the radiance and irradiance data products.